Thermal Reproducibility and Voltage Stability of Carbon Black/Multiwalled Carbon Nanotube and Carbon Black/SnO_2-Sb Coated Titanium Dioxide Filled Silicone Rubber Heaters

Gwang-Tae Kim, Eun-Soo Park

Young Chang Silicone Co., Ltd., 481-7 Gasan-Dong, Kumchun-Gu, Seoul 153-803, Korea

Received 4 November 2007; accepted 7 February 2008
DOI 10.1002/app.28200
Published online 17 April 2008 in Wiley InterScience (www.interscience.wiley.com).

ABSTRACT: Flexible heaters were prepared by extruding platinum-catalyzed silicone rubber (SR) compound with carbon black (CB)/multiwalled carbon nanotube (MWNT) and CB/SnO_2-Sb coated titanium dioxide (TiO_2). MWNT with average particle length of 20 μm and acicular shaped TiO_2 with average particle length of 1.7 μm were selected. Thermal aging and mechanical deformation stability were compared for SR/CB, SR/CB/MWNT, and SR/CB/TiO_2 composites system. During thermal aging, conductor resistivity decreased because of the toughening effect of SR matrix. When 1 wt % of MWNT and TiO_2 were added into SR/CB compound, the deformation stability increased significantly. Thermal reproducibility and voltage stability of the extruded heaters were also investigated by applying AC voltage of 220 V. The heaters containing MWNT exhibited poor thermal reproducibility and voltage stability compared with heater containing TiO_2 or unfilled. © 2008 Wiley Periodicals, Inc. J Appl Polym Sci 109: 1381–1387, 2008

Key words: elastomers; extrusion; fillers; matrix; silicone rubber

INTRODUCTION

Elastomers loaded with electrically conductive fillers are commonly used as contact point materials, for electrostatic charge dissipation, as surface heaters, EMI shielding, and rubber contact switches.[1–4] However, these materials show poor reproducibility of resistivity during a long period of time or when undergoing thermal cycles.[5] Bending or other deformations can cause severe problems in conductive plastics and elastomers utilized as resistors, strain measuring devices,[6] or heating elements.[7,8]

Chaki and coworkers[9] reported that silicone compound containing acetylene black and short carbon fiber showed a high level of electroconductivity and the percolation region for conduction appeared at much lower concentration compared with acrylonitrile butadiene rubber and ethylene–propylene–diene monomers, especially when carbon fiber was used as conductive filler.

Park et al.[4] demonstrated that carbon black (CB)/copper powder filled flexible silicone rubber (SR) heaters exhibited excellent thermal and electrical reproducibility. However, metallic powders generally suffer from oxidation and the corresponding deterioration of the electrical properties of the composite comes from the nonconductive nature of such oxide layers. It is also reported that SnO_2-Sb coated titanium dioxide (TiO_2) improved positive temperature coefficient (PTC) effect and electrical properties of SR/CB composite significantly.[10] Many efforts were tried to improve the electrical stability of polymeric electroconductive materials.[10–13]

Carbon nanotube (CNT) is recognized as the ultimate carbon fibers for high performance and multifunctional composites because of their high mechanical strength, high thermal stability in air, good electrical properties, and high thermal conductivity.[14–17] In this study, flexible heaters were extruded with SR/CB, SR/CB/multiwalled carbon nanotube (MWNT), and SR/CB/TiO_2 compounds. The effect of thermal aging and mechanical deformation on the electrical resistivity of prepared heaters was evaluated. Thermal reproducibility and voltage stability of polytetrafluoroethylene (PTFE) tape insulated heaters were also investigated during applying AC voltage of 220 V.

EXPERIMENTAL

Materials

Platinum-catalyzed SR (dilution SR; PT2760; Tail Chemical, Korea) and electroconductive platinum-

Correspondence to: E.-S. Park (t2phage@hitel.net).

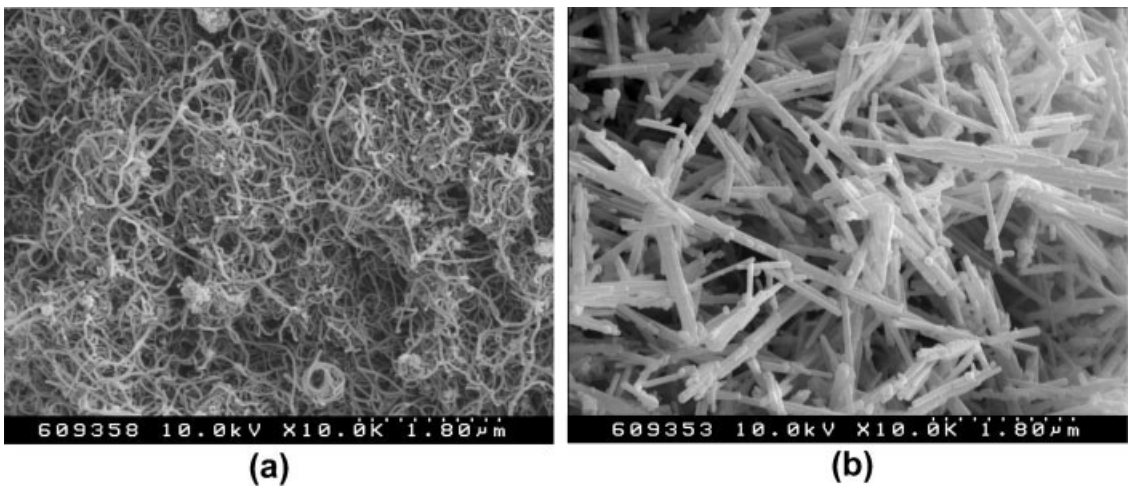

Figure 1 SEM images of the MWNT and SnO_2-Sb coated titanium dioxide.

catalyzed SR [PT374 (CB content 36.0 wt %); Tail Chemical] were used as received. Electroconductive TiO_2 [FT1000 (diameter: 130 nm; length: 1.7 μm; specific gravity: 4.4); Ishihara Sangyo Kaisha, Korea] and MWNT [CM-95 (purity: 95 wt %; diameter: 15 nm; length: 20 μm; specific gravity: 1.8); Iljin CNT, Korea] were used as received. FT series TiO_2 is based on rutile type of TiO_2 whose surface is coated with a thin electroconductive SnO_2-Sb layer.

Compounding of electroconductive SR

The electroconductive SR (50 g) and dilute SR (71 g) were premixed using a two-roll mill at room temperature for 5 min followed by MWNT (1 g) being slowly added to the flux roll. The compound band was then sheeted, folded, and rebanded for mixing. This process was repeated 30 times to ensure thorough mixing.

Instrumentation

Scanning electron microscopy (SEM) observations of the conductive fillers were performed on a Hitachi *S*-4200 model. The specimens were prepared by a coating with gold in an SPI sputter coater. The morphology was determined using an accelerating voltage of 10 kV.

Hardness of the specimens was measured with a Shore A type hardness tester (GS-706; Teclock, Japan) and the readings averaged. Five locations were measured for each specimen and surface.

Tensile test procedure

Dumbbell specimens for mechanical tests were prepared in accordance with ASTM D 412 specification. Tensile properties of samples were determined with a universal test machine (UTM, Model DECMC00; Dawha Test Machine, Korea) at a cross head speed of 500 mm min^{-1}. The mean value of at least five specimens of each sample was taken, although specimens that broke in an unusual manner were disregarded.

Measurement of volume resistivity

Platinum-catalyzed SR and MWNT were compounded with a two-roll mill at room temperature for 20 min. The milled rubber sheet (100 × 100 × 2.5 mm^3) was fed into a compress mold cavity (150 × 150 × 1 mm^3). The mold was placed between two stainless-steel platens and heated in a 185°C hot press at a pressure of 10 atm for 10 min. When the curing process finished, the platens and mold were cooled to room temperature. The cured films had a thickness of 1.2 ± 0.2 mm. Resistivity of the specimens was measured by Wheatstone bridge (2755,

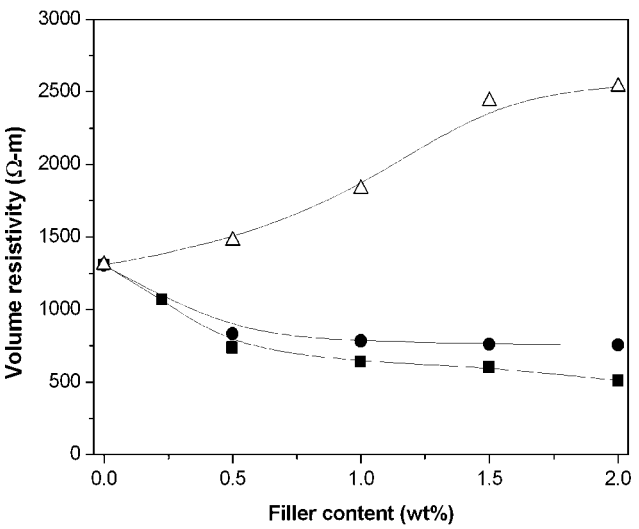

Figure 2 ρ_v as a function of the CB, MWNT, and TiO_2 content. (■) SR/CB, (●) SR/CB/MWNT, (△) SR/CB/TiO_2.

TABLE I
Volume Resistivity of the SR/CB, SR/CB/MWNT, and SR/CB/TiO_2 Composites

	Volume resistivity, ρ_v (Ω cm)				
Sample code	64.0/36.0[a]	82.0/18.0[a]	84.6/15.4[a]	84.4/14.6[a]	85.5/14.5[a]
SR/CB	2	80	600	1070	1310
	85.6/14.4/0.5[a]	85.6/14.4/1.0[a]		85.6/14.4/1.5[a]	85.6/14.4/2.0[a]
SR/CB/MWNT	830	785		760	755
SR/CB/TiO_2	1470	1830		2440	2540

[a] Concentration of the composites (wt %).

Portable Wheatstone Bridge; Yokogawa, Japan) according to KSM 6773 (Testing method for volume resistivity of electrically conductive rubber and plastic materials, 1989) at 20°C ± 1°C. Volume resistivity (ρ_v) of prepared films was calculated by using the following equation:

$$\rho_v = \frac{AR_v}{L}$$

where A, R_v, and L represent the area of the effective electrode (cm^2), measured resistance (Ω), and distance between electrodes (cm), respectively.

Extrusion of heater

The heater was composed of conductor and heating layer. The heating layer is applied to the tinned annealed copper conductor by extrusion with electroconductive compound. All heaters were extruded at a speed of 100 rpm using a single screw extruder [SH2001-100 (maximum loading capacity: 70 kg h^{-1}); Sung Heuy Industry, Korea] equipped with a dumbbell shaped die (7.9 × 2.1 mm^2) and a 1 : 10 compression ratio screw. Extruded samples were cured by passage through a heating box at 450°C with a curing rate of 10 m min^{-1}.

Conductor resistivity measurement of extruded heaters

Conductor resistivity (ρ_c) is defined as resistivity between the conductors of an extruded heater per meter (Ω m^{-1} of heater). ρ_c was measured by using a digital multimeter (3234 Card Hitester; Saehan, Korea). Each electrical probe of the multimeter was connected to the heater's conductor using a cable and resistivity measurements were conducted at 20°C ± 1°C. The measurements of ρ_c versus temperature behavior were conducted in a convection oven from 20 to 200°C at a heating rate of 20°C min^{-1}.

Deformation stability test of heater

The extruded heater was strained at a speed of 5 mm min^{-1} using the UTM. Each electrical probe of the multimeter was connected to the heater's conductor using a cable and resistivity measurements were conducted at 20°C ± 1°C.

RESULTS AND DISCUSSION

Figure 1 shows the SEM image of conductive fillers. MWNT produced by a chemical vapor deposition process, with an average diameter of about 15 nm and average length of 20 μm. Electroconductive TiO_2 was acicular shaped TiO_2 coated with a thin conductive SnO_2-Sb layer. Average diameter and average length of TiO_2 were 130 nm and 1.7 μm, respectively.

Figure 2 represents the volume resistivity (ρ_v) of the SR/CB, SR/CB/MWNT, and SR/CB/TiO_2 composites as a function of conductive filler content in Table I. The ρ_v of composites decreased in order of SR/CB/TiO_2 > SR/CB/MWNT > SR/CB. Electrical resistivity change depends on the polymer matrix

TABLE II
Tensile Properties of SR/CB, SR/CB/MWNT, and SR/CB/TiO_2 Composites

Sample code	SR/CB/filler content (wt %)	Tensile properties		
		Tensile strength (MPa)	Elongation at break (%)	Hardness (Shore A)
SR/CB14.9	85.1/14.9/0.0	6.5 ± 0.3	538 ± 24	60
SR/CB15.9	85.1/14.9/1.0	7.6 ± 0.2	527 ± 51	61
SR/CB14.9/MWNT1.0	85.1/14.9/1.0	7.1 ± 0.3	484 ± 19	63
SR/CB14.9/$TiO_2$1.0	85.1/14.9/1.0	7.1 ± 0.2	463 ± 50	61

and formation of conducting pathways through the filler phase. Owing to small amount of MWNT or TiO_2 were mixed with SR/CB compound, they come into use making the contact point with CB aggregates rather than making the conductive pathway themselves.

Table II demonstrates the tensile properties of SR/CB, SR/CB/MWNT and SR/CB/TiO_2 composites. Addition of CB, MWNT and TiO_2 led to the increase in both tensile strength and hardness whereas that led to decrease in elongation at break. Small particles size and high aspect ratio allow the filler particles to act as barriers to the propagation of microcracks and provide the higher tensile strength required to resist failure. In contrast the introduction of filler into the elastomer provides additional hardness and resistance to elongation.

Dumbbell-shaped heaters were extruded with SR/CB14.9 compound containing 1 wt % of MWNT or TiO_2. Figure 3 represents a fractured surface of extruded SR/CB14.9, SR/CB14.9/MWNT1.0, and CB14.9/TiO_2 compounds. In the case of MWNT and TiO_2 containing compounds, no morphological change was shown, compared with SR/CB. Unfortunately, it is difficult to form stable dispersions of nanoparticles in polymer matrices, and proper characterization of these materials is complicated by the fact that physically relevant length scales range from macroscopic to molecular dimensions.[17,18] Table III summarizes the properties of extruded heaters. The conductor resistivity (ρ_c) is defined as the resistivity between the conductors measured at 20°C. It is noted that the ρ_v of the compression-molded SR/CB compound is lower than that of SR/CB/MWNT in Table I. In contrast, the ρ_c of the extruded heaters decreased in order of SR/CB/TiO_2 > SR/CB > SR/CB/MWNT. In compression-molded composites, MWNT are randomly arranged in all three directions and do not effectively make the contact point with CB aggregates. For extruded composite, high aspect ratio particles tend to align in the direction of extrusion flow[19] (Fig. 3) and they are easily making the conductive pathway parallel to the conductors. The heater-output characteristics were measured in the heater surface temperature at applied voltage AC of 220 V, as shown in Table III. The heaters can be used in heater-output range from 47 to 117°C in both general and high-output purpose.

Figure 4 indicates resistivity temperature behavior of the extruded heaters. Polymeric electroconductive material shows a temperature coefficient of resistance. Temperature coefficient of resistance is defined as the amount of change of the resistance of a material for a given change in temperature. A PTC indicates that resistance increases with temperature; a negative temperature coefficient (NTC) indicates that resistivity decreases with temperature.[11] The resistivity–temperature behavior of all heaters exhibited PTC effect without NTC effect. PTC phenomenon is attributed to the separation of conductive pathways by thermal volume expansion, that is, because of the

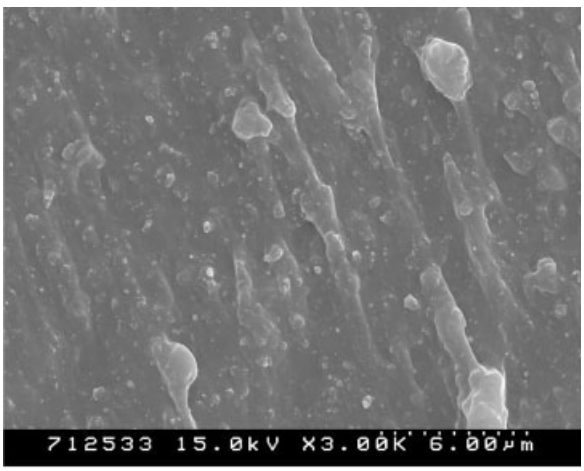

(a) SR/CB14.9

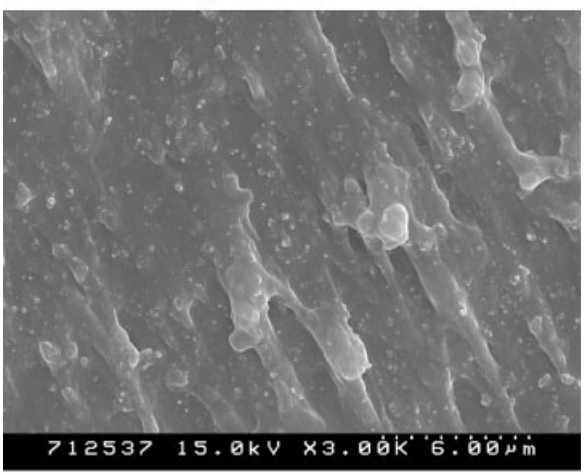

(b) SR/CB14.9/MWNT1.0

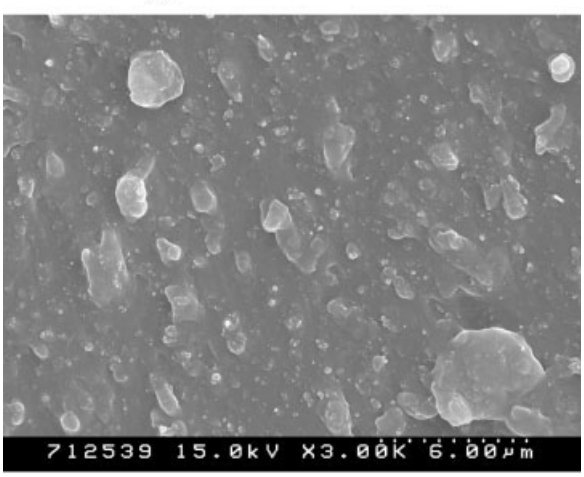

(c) SR/CB14.9/$TiO_2$1.0

Figure 3 SEM images of the extruded SR/CB14.9, SR/CB14.9/MWNT1.0, and CB14.9/$TiO_2$1.0 compound.

TABLE III
Characterization of the Extruded Heaters

Sample code	SR/CB/filler content (wt %)	Conductor resistivity, ρ_c (Ω)	Output[a] at 220 V, 25°C (W/m)	Maximum heater-output temperature (°C)
Heater-CB14.0	86.0/14.0/0.0	3450	14	47
Heater-CB14.4	85.6/14.4/0.0	680	71	87
Heater-CB14.9	85.1/14.9/0.0	230	210	101
Heater-CB14.9-MWNT1.0	85.1/14.9/1.0	110	440	114
Heater-CB14.9-$TiO_2$1.0	85.1/14.9/1.0	300	161	86

[a] Measured by initial ρ_c.

difference in the expansion coefficient between the polymer matrix and the conductive filler.[20] As the conductive filler content of heaters is increased, the rate of increase in resistivity was decreased. With the increase in conductive filler loading, there is an increase in the number of conductive networks and average interparticle gap becomes smaller. As a result, the contact pressure of particle becomes higher for higher conductive filler loading and the network breakdown process becomes less efficient.

Figure 5 shows the relative resistivity (ρ_r) change of the extruded heaters during the mechanical deformation experiments. Here the ρ_r is defined as the ratio of the ρ_c value to the corresponding value at 20°C. The ρ_r change slightly increased for the first 0.25% strain. After this initial increase, ρ_r reached a plateau and then rapidly increased. The phenomena can generally be explained in terms of destruction of CB conductive network, decrease of conductor distance, and rupture of conductor-SR bonds. Destruction of the CB network reduced the flow of electrons and increased the microscopic resistance. The plateau state could be explained on the equilibrium of the decrease in ρ_c due to the conductors approaching and increase in ρ_c due to the destruction of CB network. Finally, when conductor-SR bonds begun to break, the resistivity of heater increases rapidly. It is found that ρ_r change of Heater-CB14.9MWNT1.0 and Heater-CB14.9$TiO_2$1.0 maintained equilibrium at 3% strain, whereas Heater-CB14.9 maintained equilibrium at 1.5%. The addition of MWNT and TiO_2 into SR/CB compound improved the polymeric deformation stability significantly because of the increase in resistivity switching effect.

Figure 6 demonstrates the ρ_c changes of the extruded heaters after thermal aging at 250°C. During the thermal aging, ρ_c decreased significantly further at 140 min and almost remained at this level. The initial decrease in ρ_c of the heaters after thermal aging is attributed to the decrease in resistivity between the conductors and CB particles in the composites and to the decrease in low molecular weight components, such as oligomers, catalyst byproducts, and volatile residues. Thermal aging of the heaters toughened the SR matrix, which increased the contact pressure between the conductive particles, and thereby the

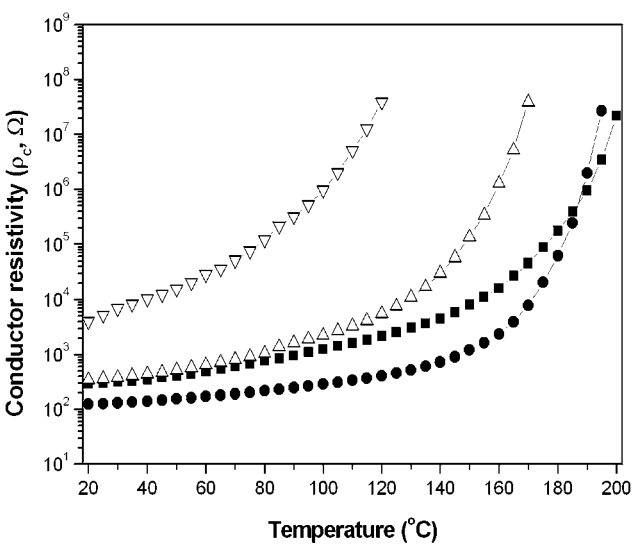

Figure 4 Resistivity–temperature behavior of the extruded heaters. (■) Heater-CB14.9, (●) Heater-CB14.9-MWNT1.0, (△) Heater-CB14.9-$TiO_2$1.0, (▽) Heater-CB14.0.

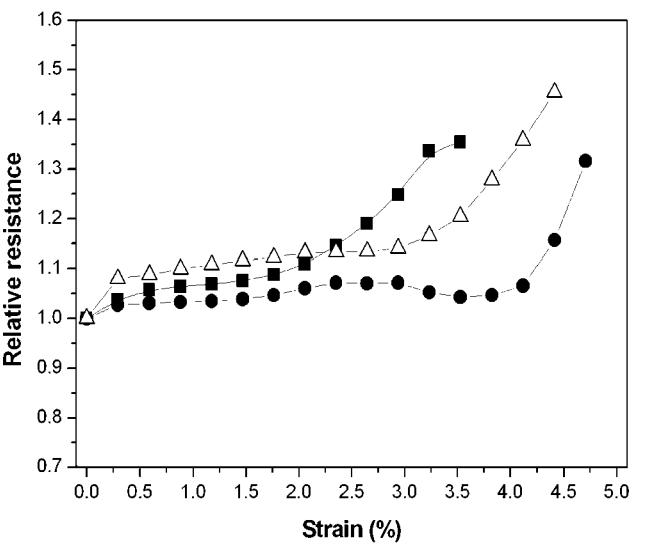

Figure 5 ρ_r changes of the extruded heaters during the deformation experiments. (■) Heater-CB14.9, (●) Heater-CB14.9-MWNT1.0, (△) Heater-CB14.9-$TiO_2$1.0.

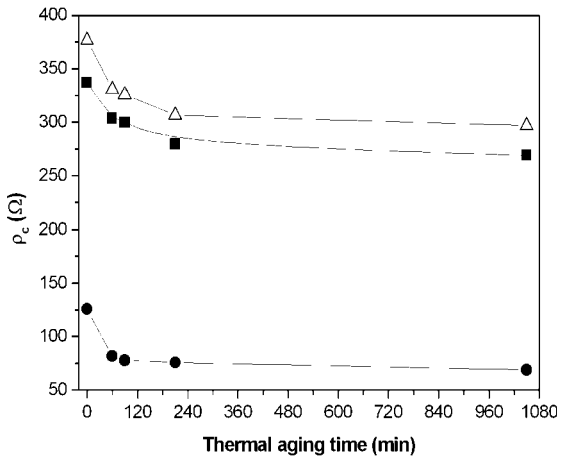

Figure 6 ρ_c changes of the extruded heater during the thermal aging. (■) Heater-CB14.9, (●) Heater-CB14.9-MWNT1.0, (△) Heater-CB14.9-$TiO_2$1.0.

total conductivity was increased. After thermal aging, all heaters maintained stable ρ_c value, which indicated that they had good thermal aging resistance.

Under long-term voltage applications, the heat-output reproducibility is one of the most important requirements for heating elements. To determine the voltage stability of heaters, PTFE tape warped heater (1 m) was wound with a steel pipe (diameter: 40 mm; thickness: 1 mm) and thermally insulated with glass cloth quipped with a temperature recorder. The heater-output changes were recorded at 1 h intervals. Figure 7 shows the results of voltage stability test of PTFE warped heaters at AC of 220 V for 196 h. Heater-CB14.9 and Heater-CB14.9$TiO_2$1.0 exhibit good voltage stability. In contrast, the heater-output of Heater-CB14.9MWNT1.0 showed a dramatic decrease after

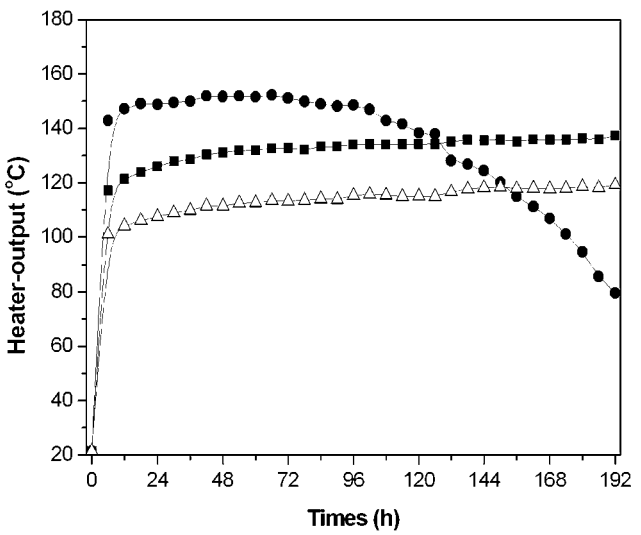

Figure 7 Heater-output changes of the PTFE insulated heaters at applied voltage of 220 V. (■) Heater-CB14.9, (●) Heater-CB14.9-MWNT1.0, (△) Heater-CB14.9-$TiO_2$1.0.

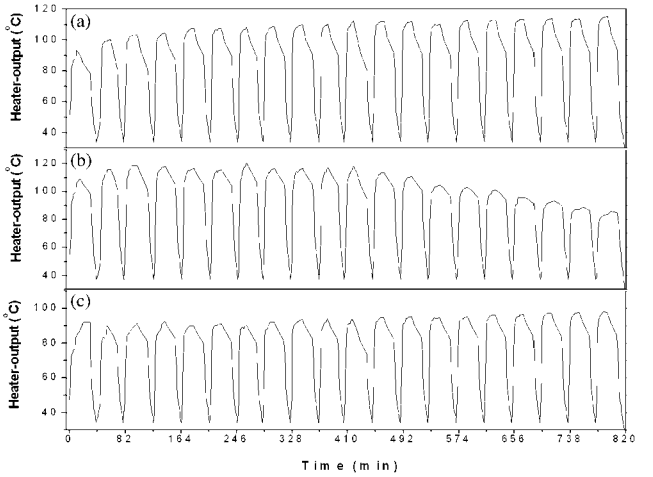

Figure 8 Cycling experiments of the PTFE insulated heaters with periodic change in applied voltage of 220 V. (a) Heater-CB14.9, (b) Heater-CB14.9-MWNT1.0, (c) Heater-CB14.9-$TiO_2$1.0.

96 h compared with Heater-CB14.9 and Heater-CB14.9$TiO_2$1.0.

Figure 8 demonstrates stability of PTFE insulated heaters subjected to heating and cooling cycles with periodic change in voltage of AC 220V. The power switch was turned off after 30 min of voltage applications. After the heater cooled down to room temperature, the voltage was applied again. Heater-output changed at an early stage of the cycling test (Heater-CB14.9 and Heater-CB14.9MWNT) because of gradual randomization of the conductive aggregates and then approached to a maximum value owing to rebuilding of the conductive network previously destroyed during the heating step. It is found that significant heater-output reproducibility was exhibited by Heater-CB14.9$TiO_2$1.0. In contrast, Heater-CB14.9MWNT1.0 shows a decrease of heater-output after the 10th individual run during the cycling test. The heater-output loss of Heater-CB14.9MWNT1.0 from voltage stability and cycling test is the result of increased internal resistance caused by electrochemical oxidation of CNT and CB. MWNT deposits contain the impurities such as metallic catalyst particles and carbonaceous materials.[15] In the case of long-term or cyclic voltage applied MWNT containing heater, the metallic impurities accelerate the electrochemical oxidation of CNT and CB. Finally, the heater loses initial conductivity, and heater-output is gradually declined.

CONCLUSIONS

PTC heaters were prepared by extruding with SR/CB/MWNT and SR/CB/TiO_2 composite. The effect of thermal aging and mechanical deformation on the electrical resistivity of prepared heaters was evaluated.

After thermal aging process, all heaters maintained stable ρ_c value, which indicated that they had good thermal aging resistance. To measure the mechanical stability, the extruded heater was strained at a speed of 5 mm min^{-1} using the UTM. The addition of MWNT and TiO_2 into SR/CB compound improved the mechanical deformation stability significantly.

Voltage stability and thermal reproducibility of the PTFE insulated heaters were also investigated by applying a AC voltage of 220 V. A significant voltage stability and thermal reproducibility was exhibited by the heater containing TiO_2. Addition of acicular-shaped filler enhanced the stability of conducting pathway because of the increase of the contact point between the conductive particles without reducing the thermoelectric switching effect. In contrast, heaters containing MWNT has poor voltage stability and thermal reproducibility because of electrochemical oxidation caused by the metallic impurities in MWNT.

References

1. Norman, R. H. Conductive Rubbers and Plastics; Elsevier: Amsterdam, 1970.
2. Bigg, D. M. Polym Eng Sci 1979, 19, 1188.
3. Park, E. S.; Yun, S. J.; Kim, G. T; Park, I. J.; Choi, W. H.; Jeong, J. W.; Hong, S. Y.; Park, H. W.; Jang, L. W.; Yoon, J. S. J Appl Polym Sci 2004, 94, 1611.
4. Park, E. S.; Jang, L. W.; Yoon, J. S. J Appl Polym Sci 2005, 95, 1122.
5. Kost, J. M.; Narkis, A.; Foux, A. J Appl Polym Sci 1984, 29, 3937.
6. Zheng, Q.; Song, Y.; Wu, G.; Song, X. J Polym Sci Part B: Polym Phys 1993, 50, 1891.
7. Narkis, M. Mod Plast 1983, 60, 96.
8. Narkis, M.; Vaxman, A. J Appl Polym Sci 1984, 29, 1639.
9. Sau, K. P.; Khastgir, D.; Chaki, T. K. Angew Makromol Chem 1998, 258, 11.
10. Park, E. S. Macromol Mater Eng 2006, 291, 690.
11. Park, E. S. Macromol Mater Eng 2005, 290, 1213.
12. Shen, L.; Lou, Z. D.; Qian, Y. J. J Polym Sci Part B: Polym Phys 2007, 45, 3078.
13. Pourabbas, B.; Peighambardoust, S. J. J Appl Polym Sci 2007, 105, 1032.
14. Harris, P. J. F. Int Mater Rev 2004, 49, 31.
15. Peigney, A.; Flahaut, E.; Laurent, Ch.; Chastel, F.; Rosset, A. Chem Phys Lett 2002, 352, 20.
16. Flahaut, E.; Peigney, A.; Laurent, Ch.; Marliere, Ch.; Chastel, F.; Rosset, A. Acta Mater 2000, 48, 3803.
17. Nalwa, H. Handbook of Nanostructured Materials and Nanotechnology, Vol. 5; Academic Press: San Diego, 2002.
18. Huang, Y. Y; Ahir, S. V.; Terentjev, E. M. Phys Rev B 2006, 73, 125422.
19. Park, E. S. J Appl Polym Sci 2007, 105, 460.
20. Jing, X.; Zhao, W.; Lan, L. J Mater Sci Lett 2000, 19, 377.